FFA

FLYGTEKNISKA FÖRSÖKSANSTALTEN

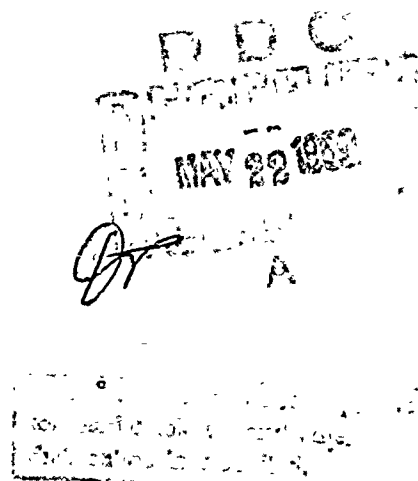### THE AERONAUTICAL RESEARCH INSTITUTE OF SWEDEN

MEDDELANDE 105

REPORT 105

VORTEX LATTICE METHOD FOR CALCULATION OF QUASI STEADY STATE LOADINGS ON THIN ELASTIC WINGS IN SUBSONIC FLOW

BY

Sven G. Hedman

STOCKHOLM 1966

VORTEX LATTICE METHOD FOR CALCULATION OF QUASI STEADY STATE LOADINGS ON THIN ELASTIC WINGS IN SUBSONIC FLOW[1]

by

Sven G. Hedman

SUMMARY

Wing systems that contain several wing surfaces are considered. The surfaces are arbitrarily divided in the chordwise and spanwise directions into panels ("boxes"). The panel load is simulated by a horseshoe vortex, and the boundary condition is fulfilled on every panel at one point. For each surface the vortices and the control points are positioned on a wing chord plane. These planes are perpendicular to the y- or z-axis. The incidence distribution or the load distribution may be found from a system of linear equations, when one of these distributions is given. The calculations can be performed for elastic wings, if the elastic properties are known in the form of a deformation matrix.

The calculation procedure has been programmed for an electronic computer. Good correlation has been obtained between the results from this method and those from other lifting surface methods or experiments.

Stockholm, October 1965

WIRBELNETZVERFAHREN FÜR DIE BERECHNUNG VON QUASISTATIONÄREN BELASTUNGEN AN DÜNNEN UND ELASTISCHEN TRAGFLÄCHEN BEI UNTERSCHALLSTRÖMUNG

von

Sven G. Hedman

ZUSAMMENFASSUNG

Es werden Tragflügelsysteme betrachtet, die aus mehreren Flügelflächen bestehen. Die Flächen werden in Profilsehnenrichtung und in Richtung der Spannweite beliebig in Felder (boxes) unter[.].ilt. Die Feldbelastung wird durch einen Hufeisenwirbel nachgebildet und die Randbedingungen werden in jedem Feld an einem Punkt erfüllt. An jeder Fläche sind die Wirbel und die Aufpunkten auf einer Flügelsehnenfläche angeordnet. Diese Flächen stehen senkrecht zur y- oder z-Achse. Die Anstellwinkelverteilung oder die Lastverteilung kann aus einem System linearer Gleichungen gefunden werden, wenn eine dieser Verteilungen gegeben ist. Die Berechnungen können für elastische Flügel durchgeführt werden, sofern die elastischen Eigenschaften in Form einer Formänderungsmatrize bekannt sind.

Der Rechenvorgang wurde für einen Rechenautomat programmiert. Die Ergebnisse dieser Methode stimmen gut mit jenen anderer Tragflächenberechnungen oder Versuchen überein.

MÉTHODE A LATTIS DE TOURBILLON POUR LE CALCUL DE CHARGES QUASI STABLES SUR AILES DÉFORMABLES ET MINCES EN RÉGIME SUBSONIQUE

par

Sven G. Hedman

RÉSUMÉ

Les systèmes de voilure comportant plusieurs surfaces d'ailes sont pris ici en considération. Les surfaces sont arbitrairement divisées longitudinalement et transversalement en panneaux. La charge du panneau est simulée par un tourbillon lié et deux tourbillons libres et la condition limite est appliquée en un point de chaque panneau. Pour chaque surface, les tourbillons et les points de contrôle sont positionnés selon un plan référence de l'aile. Ces plans sont perpendiculaires aux axes y eu z. La distribution d'incidence ou la distribution de charge peuvent être trouvées grâce à un système d'équations linéaires à condition que l'une des deux distributions soit donnée. Les calculs peuvent être effectués pour des ailes déformables si les propriétés d'élasticité sont connues sous forme d'une matrice de déformation.

Les procédés de calcul ont été programmés pour une calculatrice électronique. Une bonne corrélation existe entre les résultats obtenus par cette méthode et ceux obtenus par d'autres méthodes ou des essais.

CONTENTS

DISCLAIMER NOTICE

THIS DOCUMENT IS BEST QUALITY
PRACTICABLE. THE COPY FURNISHED
TO DTIC CONTAINED A SIGNIFICANT
NUMBER OF PAGES WHICH DO NOT
REPRODUCE LEGIBLY.

VORTEX LATTICE METHOD FOR CALCULATION
OF QUASI STEADY STATE LOADINGS
ON THIN ELASTIC WINGS IN SUBSONIC FLOW

by

Sven G. Hedman

1. INTRODUCTION

In the literature a great number of methods are available for the approximate calculation of load distributions on wings in subsonic flow. Most of these methods were constructed before the arrival of the automatic computer, and thus the number of unknowns had to be kept low. This was accomplished by assumptions on the chordwise and spanwise load distributions. These assumptions were well founded for a majority of wing designs. One of these methods was the vortex lattice method of Faulkner. However, with the electronic computer available, the number of unknowns in a system of equations can be permitted to rise considerably, and therefore the assumptions on load variations are unnecessary, and, as they are not always suitable, it is better to avoid them.

This report describes an elementary method for load calculations. Let the continuous vortex distributions, which represent the continuous loading on the lifting surfaces, be replaced by a system of discrete vortices. The strengths of the vortices are determined by the requirement of tangential flow in as many points, control points, as there are vortices. The system can be thought of as a collection of horseshoe vortices. Each horseshoe vortex induces the same flow field as an elemental lifting area of the wing, a panel, does. For each wing surface the vortices and the control points are positioned on a wing chord plane.

Because the panels can be laid out in rather arbitrary patterns, the boundary condition can be fulfilled on any planform.

However, the proposition that the vortices are arranged in planes, limits the method to problems with such incidences that no vortex roll up exists over the leading edges, and that the trailing vortex sheets are close to their original wing chord planes.

2. NOTATIONS

b y-coordinate of the leading edge of wing part, $2b_{max}$ equals span
C_D drag coefficient
C_L lift coefficient
C_l rolling moment coefficient
C_m pitching moment coefficient
C_p local lift coefficient
C_n yawing moment coefficient
C_Y side force coefficient
c wing chord
h half the width of horseshoe vortex
L' spanwise loading coefficient
P, Q, R aerodynamic influence coefficients
p rate of roll
q dynamic pressure or rate of pitch
s area of wing panel
S_1 matrix of aerodynamic influence coefficients
u, v, w components of disturbance velocity along x, y, z-axis, respectively
V free-stream velocity
x, y, z Cartesian coordinates
α wing angle of attack
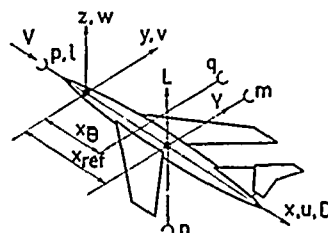
β $\sqrt{1-M^2}$, where M is Mach number

Γ vortex intensity

δ wing camber

θ $2q \cdot (x_D - x_0)/c_{ref}$

λ angle of sweep of bound vortex

ϱ density of air

ϕ py/b_{max}

ω $\alpha + \delta + \theta + \phi$ panel angle of attack

SUBSCRIPTS

D control point

V vortex

3. FLOW MODEL

The lifting system may consist of several wings, or it can be the horizontal projection of a complete airplane.

For the derivation of the formulas relating incidence and load, the lifting surfaces will be replaced by a number of plane quadrilaterals or panels. Thus the planform of the original system will be approximated by polygons, and the angle of attack distributions of the surfaces will be expressed through the incidences of the plane panels.

The load carried by one of these panels induces a flow field that can be calculated with the aid of a horseshoe vortex. The bound vortex will be positioned on the panel's quarter chord line for reasons outlined in Appendix 1. The control point, where the condition of tangential flow is satisfied, will be positioned on the three quarter chord line of the panel and halfway between that line's inboard end and outboard end. For each wing the vortices and control points will be in a representative wing chord plane, perpendicular to the y-axis for a vertical tail and to the z-axis for a wing. The free vortices are taken parallel to the x-axis.

At every control point, the normal velocity induced by all the vortices must cancel the normal component of the free stream flow. The induced velocities are calculated according to Biot-Savart's law. As the free vortices are assumed to be parallel with the x-axis, the equations for the induced velocities will be linear in the vortex intensities.

4. GEOMETRY OF THE WING PANELS

The method is not very sensitive to the pattern of panels chosen to represent the wing, except that panels behind each other should be in streamwise columns. Otherwise a control point of one panel may lie very close to the trailing vortex of another panel, where the induced velocity is high and not representative of the average induced velocities in the range between the trailing vortices.

The horseshoe vortex is geometrically defined by the coordinates x_V, y_V, z_V, h, λ, and a control point by x_D, y_D, z_D, as shown in Fig. 1.
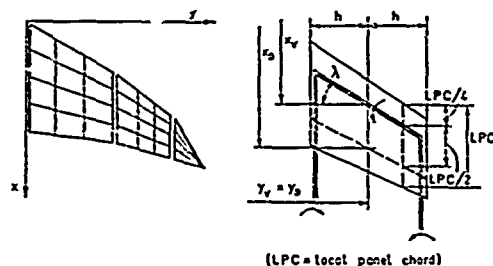

(LPC = local panel chord)

Fig. 1. Wing divided into panels and panel with vortex.

Rather than determining all these coordinates manually, it is advisable to define the input for the calculations through the major dimensions of the wing and the number of columns and rows of panels. The scheme in Appendix 2 may then be followed for the determination of the coordinates for vortices and control points.

The slope of a panel, ω, is composed of several items. The stationary contributions are the reference angle of attack, α, which is assumed to have one value for the whole lifting system, and the camber distribution or aileron deflection δ.

Quasi steady contributions appear for a rotating airplane. Let $\dot{\theta}$ be the angular velocity of rotation around the axis $x = x_0$, $z = 0$. At a point x_D, y_D, z_D the normal velocity due to rotation is $-\dot{\theta} \cdot (x_D - x_0)$. The corresponding load is the same as for a stationary surface so cambered that the normal velocity is $-\dot{\theta} \cdot (x_D - x_0)$. Let θ be the panel incidence that corresponds to a

rotation around the pitch axis (in $x = x_\theta$), and ϕ the incidence corresponding to a steady roll.

$$\left.\begin{array}{l} \theta = \dfrac{\dot{\theta} \cdot (x_D - x_\theta)}{V} = q \dfrac{x_D - x_\theta}{c_{ref}} 2 \\[3mm] \phi = \dfrac{\dot{\phi}\, y}{V} = p \dfrac{y}{b_{max}} \end{array}\right\} \quad (1)$$

where $\dot{\theta}$ and $\dot{\phi}$ are positive for a sinking trailing edge and a sinking starboard tip respectively. q and p are the dimensionless rates of pitch and roll resp., and b_{max} is the wing half span.

$$q = \dot{\theta}\, c_{ref}/(2\,V)$$

$$p = \dot{\phi}\, b_{max}/V$$

The total panel incidence ω is obtained through summation

$$\omega = \alpha + \delta + \theta + \phi$$

Angles are positive, when $dz/dx < 0$.

5. AERODYNAMICS OF A SET OF PANELS

The expression for the vortex induced flow field is derived with the aid of Biot-Savart's law which implies direct application only to incompressible flow. However, if the Prandtl-Glauert rule is accepted, the validity of the derivation can be extended to all subcritical Mach numbers.

Appendix 3 is a derivation of the formulas which give the induced velocity components u, v, w in incompressible flow at a point $(x_D, \beta y_D, \beta z_D)$ due to a horseshoe vortex strength Γ_j at $(x_V, \beta y_V, \beta z_V)$.
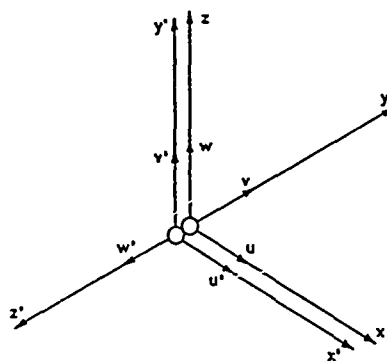
$$\left\{\begin{array}{l} u_{ij} = P_{ij}\Gamma_j \\[2mm] v_{ij} = Q_{ij}\Gamma_j \\[2mm] w_{ij} = R_{ij}\Gamma_j \end{array}\right. \quad (2)$$

The influence coefficients P, Q, R depend on the geometry of the horseshoe vortex and on the position of the downwash point relative to the vortex. The coefficients are calculated with Eq. (A3.1). The total induced velocity components are obtained

through summation over all the vortices. Let there be n of them on planes parallel to the x, y-plane.

$$\left\{\begin{array}{l} u_i = \displaystyle\sum_{j=1}^{n} u_{ij} = \sum_{j=1}^{n} P_{ij}\Gamma_j \\[4mm] v_i = \displaystyle\sum_{j=1}^{n} v_{ij} = \sum_{j=1}^{n} Q_{ij}\Gamma_j \\[4mm] w_i = \displaystyle\sum_{j=1}^{n} w_{ij} = \sum_{j=1}^{n} R_{ij}\Gamma_j \end{array}\right. \quad (3)$$

A cruciform configuration may carry load on both horizontal and vertical surfaces. Let $m - n$ be the number of vertical surface vortices. To avoid introducing a further set of equations to calculate the influence coefficients for these vortices, an x', y', z'-coordinate system will be inserted according to the sketch below.

$$\left.\begin{array}{l} u_{ij} = u'_{ij} = P'_{ij}\Gamma_j \\[2mm] v_{ij} = -w'_{ii} = -R'_{ij}\Gamma_j \\[2mm] w_{ij} = v'_{ij} = Q'_{ij}\Gamma_j \end{array}\right\} \, n + 1 \leqslant j \leqslant m$$

The primed influence coefficients are obtained from Eq. (A3.1), if y and z from the configuration are inserted into the equations in the places of $-z$ and y respectively. The total induced velocity for a cruciform configuration is obtained through summation over all the m vortices.

$$\left\{\begin{array}{l} u_i = \displaystyle\sum_{j=1}^{n} P_{ij}\Gamma_j + \sum_{j=n+1}^{m} P'_{ij}\Gamma_j \\[4mm] v_i = \displaystyle\sum_{j=1}^{n} Q_{ij}\Gamma_j - \sum_{j=n+1}^{m} R'_{ij}\Gamma_j \\[4mm] w_i = \displaystyle\sum_{j=1}^{n} R_{ij}\Gamma_j + \sum_{j=n+1}^{m} Q'_{ij}\Gamma_j \end{array}\right.$$

The condition of tangential flow at the control points is formulated under the assumption that the surface slope $\beta\omega_i$ is small.

$$-\beta\omega_i = \frac{w_i}{V_i} = \sum_{j=1}^{n} R_{ij}\frac{\Gamma_j}{V_i} + \sum_{j=n+1}^{n} Q'_{ij}\frac{\Gamma_j}{V_i}, \quad i \leq n$$

$$-\beta\omega_i = \frac{v_i}{V_i} = \sum_{j=1}^{n} Q_{ij}\frac{\Gamma_j}{V_i} - \sum_{j=n+1}^{m} R'_{ij}\frac{\Gamma_j}{V_i},$$

$$n+1 \leq i \leq m$$

Γ will be replaced by C_p, where C_p is the coefficient for the average pressure difference between the panel's lower and upper surfaces. The area of the transformed panel is $2\beta h \cdot 2(x_D - x_V)$.

$$C_{p_j}(\text{incompr}) = \frac{\varrho V_j \Gamma_j \cdot 2\beta h_j}{\frac{1}{2}\varrho V^2 \cdot 2\beta h_j \cdot 2(x_{D_j} - x_{V_j})}$$

$$= \frac{\Gamma_j}{V} \cdot \frac{1}{x_{D_j} - x_{V_j}} \cdot \frac{V_j}{V}$$

The compressible flow pressure coefficient C_p is obtained from Prandtl-Glauert's rule.

$$C_{p_j} = \frac{1}{\beta^2} \cdot \frac{\Gamma_j}{V} \cdot \frac{1}{x_{D_j} - x_{V_j}} \cdot \frac{V_j}{V}$$

The tangential flow equations are then written in terms of pressure coefficients

$$-\omega_i = \beta\frac{V}{V_i}\left[\sum_{j=1}^{n} R_{ij}(x_{D_j} - x_{V_j})\frac{V}{V_j}C_{p_j}\right.$$

$$\left. + \sum_{j=n+1}^{m} Q'_{ij}(x_{D_j} - x_{V_j})\frac{V}{V_j}C_{p_j}\right], \quad i \leq n$$

$$-\omega_i = \beta\frac{V}{V_i}\left[\sum_{j=1}^{n} Q_{ij}(x_{D_j} - x_{V_j})\frac{V}{V_j}C_{p_j}\right.$$

$$\left. - \sum_{j=n+1}^{m} R'_{ij}(x_{D_j} - x_{V_j})\frac{V}{V_j}C_{p_j}\right], \quad n+1 \leq i \leq m$$

In a parallel flow field of constant velocity, $V_i = V_j = V$. For this condition these equations can be reduced to a matrix equation.

$$\{\omega\} = -\beta[S_1]\left[\begin{matrix}\searrow \\ x_D - x_V \\ \searrow\end{matrix}\right]\{C_p\}; \quad [S_1] = \left[\begin{matrix}R & \vdots & Q' \\ \cdots & & \cdots \\ Q & \vdots & -R'\end{matrix}\right]$$

$$(4)$$

The upper parts of the columns of ω and C_p contain values for the horizontal surfaces

and the lower parts values for the vertical ones. With the above equation, the camber ω can be calculated for a wing that carries the loading C_p in a compressible subsonic flow.

However, for an elastic wing, the camber will change when the wing is unloaded. The effects of elasticity are treated in Appendix 4.

The load distribution that corresponds to a given incidence distribution can be calculated after inversion of Eq. (4).

$$\{C_p\} = -\frac{1}{\beta}\left[\begin{matrix}\searrow \\ \frac{1}{x_D - x_V} \\ \searrow\end{matrix}\right][S_1]^{-1}\{\omega\} \tag{5}$$

After the pressure distribution is known, force and moment coefficients are easily summed.

$$C_L = \frac{\sum\limits_{j=1}^{n} s_j C_{p_j}}{\sum\limits_{j=1}^{n} s_j} \tag{6}$$

$$C_m = \frac{\sum\limits_{j=1}^{n} s_j \cdot (x_{\text{ref}} - x_{V_j}) C_{p_j}}{c_{\text{ref}} \sum\limits_{j=1}^{n} s_j} \tag{7}$$

$$C_Y = \frac{\sum\limits_{j=n+1}^{m} s_j C_{p_j}}{\sum\limits_{j=1}^{n} s_j}$$

$$C_n = \frac{\sum\limits_{j=n+1}^{m} s_j \cdot (x_{\text{ref}} - x_{V_j}) C_{p_j}}{2b_{\max} \sum\limits_{j=1}^{n} s_j}$$

$$C_l = \frac{\sum\limits_{j=1}^{n} s_j y_{V_j} C_{p_j} + \sum\limits_{j=n+1}^{m} s_j z_{V_j} C_{p_j}}{2b_{\max} \sum\limits_{j=1}^{n} s_j} \tag{8}$$

In these equations, s is the panel area

$$s_j = 4h_j(x_{D_j} - x_{V_j}), \tag{9}$$

x_{ref} is the reference point for pitching and yawing moments, c_{ref} is the reference length for the pitching moment coefficient, and $2b_{\max}$ (=total span) is the reference length for the rolling moment coefficient.

For many problems, the spanwise loading coefficient for unit lift coefficient is of great interest. This parameter is commonly written $(c_l \cdot c)/(C_L \cdot c_{av})$, where c_{av} is the average chord. It can also be defined as the relative change in lift due to a change in the dimensionless spanwise coordinate.

$$L' = \frac{\Delta(L/q)}{L/q} \cdot \frac{b_{max}}{\Delta y}$$

$$L'_l = \frac{b_{max} \sum_{j=s}^{t} (x_{Dj} - x_{Vj}) C_{Pj}}{\sum_{j=1}^{n} h_j \cdot (x_{Dj} - x_{Vj}) C_{Pj}}$$

where $s \leqslant j < t$ is the interval in j corresponding to the panels in column l.

From the spanwise loading, the drag coefficient is readily obtainable. Ref. 2 contains a suitable expression for symmetrically loaded wings.

$$C_D/C_L^2 = \frac{\pi \sum_{j=1}^{n} s_j}{16 \cdot b_{max}^2} \cdot [L_1'^2 + L_2'^2 + L_3'^2 + L_4'^2]/2$$

$$- L_4' \cdot (0.0561\, L_1' + 0.7887\, L_3')$$

$$- L_2' \cdot (0.7352\, L_1' + 0.8445\, L_3')]$$

L_1', L_2', L_3', and L_4' are the values of L' at the spanwise stations $y_1/b_{max} = 0.9239$, $y_2/b_{max} = 0.7071$, $y_3/b_{max} = 0.3827$, and $y_4/b_{max} = 0$, respectively.

So far no restrictions of symmetry have been made. If the problem is symmetric or antisymmetric, great savings in the amount of computation for a given accuracy can be made. For planforms that are symmetric with respect to the x,z-plane, only one half, say the starboard half, of the configuration needs to be defined geometrically.

When the camber distribution is symmetric, the vortex intensity $\Gamma_j^{(s)}$ of the j-th panel of the starboard side is the same as the vortex intensity $\Gamma_j^{(p)}$ of an equally positioned panel of the port side. The induced velocity due to such a panel pair is the sum of each panel's contribution.

Let the superscript (ss) indicate that as

well vortex as control point are situated on the starboard side. The induced velocities are written analogously to Eq. (2)

$$\begin{cases} u_{ij}^{(ss)} = P_{ij}^{(ss)} \Gamma_j^{(s)} \\ v_{ij}^{(ss)} = Q_{ij}^{(ss)} \Gamma_j^{(s)} \\ w_{ij}^{(ss)} = R_{ij}^{(ss)} \Gamma_j^{(s)} \end{cases}$$

The contribution of the port side vortex to the velocities at the starboard control point are the same as the starboard side vortex velocity contributions in a control point placed symmetrically on the port wing (except for the sign of the y-component). The latter approach is chosen because it is simpler to move the control point than the vortex from starboard to port wing half.

$$\begin{cases} u_{ij}^{(sp)} = P_{ij}^{(sp)} \Gamma_j^{(p)} = P_{ij}^{(ps)} \Gamma_j^{(s)} \\ v_{ij}^{(sp)} = Q_{ij}^{(sp)} \Gamma_j^{(p)} = - Q_{ij}^{(ps)} \Gamma_j^{(s)} \\ w_{ij}^{(sp)} = R_{ij}^{(sp)} \Gamma_j^{(p)} = R_{ij}^{(ps)} \Gamma_j^{(s)} \end{cases}$$

The influence coefficients with superscript (ss) are obtained from Eq. (A3.1), and the ones with superscript (ps) can also be obtained from that equation, if y_D in the equation is replaced by $(-y_D)$.

The total velocity components are arrived at by summation.

$$\begin{cases} u_i = \sum_{i=1}^{n} (P_{ij}^{(ss)} + P_{ij}^{(ps)}) \Gamma_j \\ v_i = \sum_{i=1}^{n} (Q_{ij}^{(ss)} - Q_{ij}^{(ps)}) \Gamma_j \\ w_i = \sum_{i=1}^{n} (R_{ij}^{(ss)} + R_{ij}^{(ps)}) \Gamma_j \end{cases}$$

n is the number of panels on one wing half. The Eqs. (4–7) can be used to solve symmetric problems, if the following statement is met:

$$\begin{cases} P_{ij} = P_{ij}^{(ss)} + P_{ij}^{(ps)} \\ Q_{ij} = Q_{ij}^{(ss)} - Q_{ij}^{(ps)} \\ R_{ij} = R_{ij}^{(ss)} + R_{ij}^{(ps)} \end{cases}$$

Let finally the camber distribution be antisymmetric, and apply the same reasoning as before. It should be recognized that $\Gamma_j^{(p)} = - \Gamma_j^{(s)}$.

$$u_i = \sum_{j=1}^{n} (P_{ij}^{(xn)} - P_{ij}^{(zn)}) \cdot \Gamma_j$$

$$v_i = \sum_{j=1}^{n} (Q_{ij}^{(yn)} \div Q_{ij}^{(yn)}) \cdot \Gamma_j$$

$$w_i = \sum_{j=1}^{n} (R_{ij}^{(xn)} - R_{ij}^{(zn)}) \cdot \Gamma_j$$

Antisymmetric cases can then be solved by Eqs. (4, 5) and (8).

$$P_{ij} = P_{ij}^{(xn)} - P_{ij}^{(zn)}$$
$$Q_{ij} = Q_{ij}^{(yn)} \div Q_{ij}^{(zn)}$$
$$R_{ij} = R_{ij}^{(xn)} - R_{ij}^{(zn)}$$

6. EXAMPLES OF CALCULATIONS

The presented method has been programmed for SAAB's computor D21. A large number of calculations has been performed. Some of them which are of general interest will be discussed.

Fig. 2 contains a comparison of the spanwise distributions of load and center of pressure calculated by the lifting line method, by several lifting surface methods, and measured by Malavard in an electric potential tank. The wing is a 45° delta wing of aspect ratio 3. The SAAB calculations were performed on a model with four rows of panels distributed over the chord and with 10 columns on the half span. Material for the comparison is taken from Refs. 3 and 4. The table in the figure shows the integrated values, lift coefficient and total chordwise center of pressure. The agreement is good.

To investigate how much the panel pattern influences the calculated values of lift coefficient and center of pressure several patterns have been chosen as input for this particular delta wing. In all cases the chords were divided into equal rows of panels, and in the five first cases the half span was divided into equally wide columns of pan-
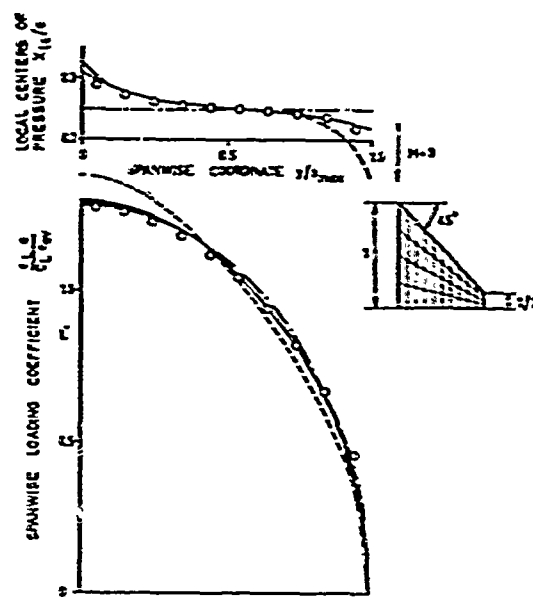
| Method	Symbol	C_{Lz}	z_{tc}/c
Lifting line	$-----$	3.6S	0.532
Lifting surface Weissinger	$- \cdot -$	3.01	0.521
Lifting surface Multhopp	$- - -$	3.06	0.535
Lifting surface Falkner	$———$	3.19	6.532
Potential tank Malavard		3.10	0.535
Vortex lattice, present method	O	3.14	0.531

Fig. 2. Loading for a delta wing. Comparison between methods.

els. In the sixth case the spanwise division was made in intervals of the angle $\pi/20$, $y = \sin (\pi n/20)$, $0 \leqslant n \leqslant 10$.

Case	Number of rows	Number of columns	Lift curve-slope	Center of pressure x-coord	Center of pressure y-coord
1	1	5	3.20	0.531	0.437
2	2	5	3.20	0.536	0.436
3	4	5	3.20	0.538	0.436
4	8	5	3.20	0.539	0.435
5	4	10	3.14	0.534	0.429
6	4	10	3.17	0.534	0.428

All values are within 2 % of one another.

Measured and calculated loadings are compared in Fig. 3 for a delta wing configuration in a $M = 0.7$ air stream. In the calculations the body was not considered. Instead the exterior wing was extended to
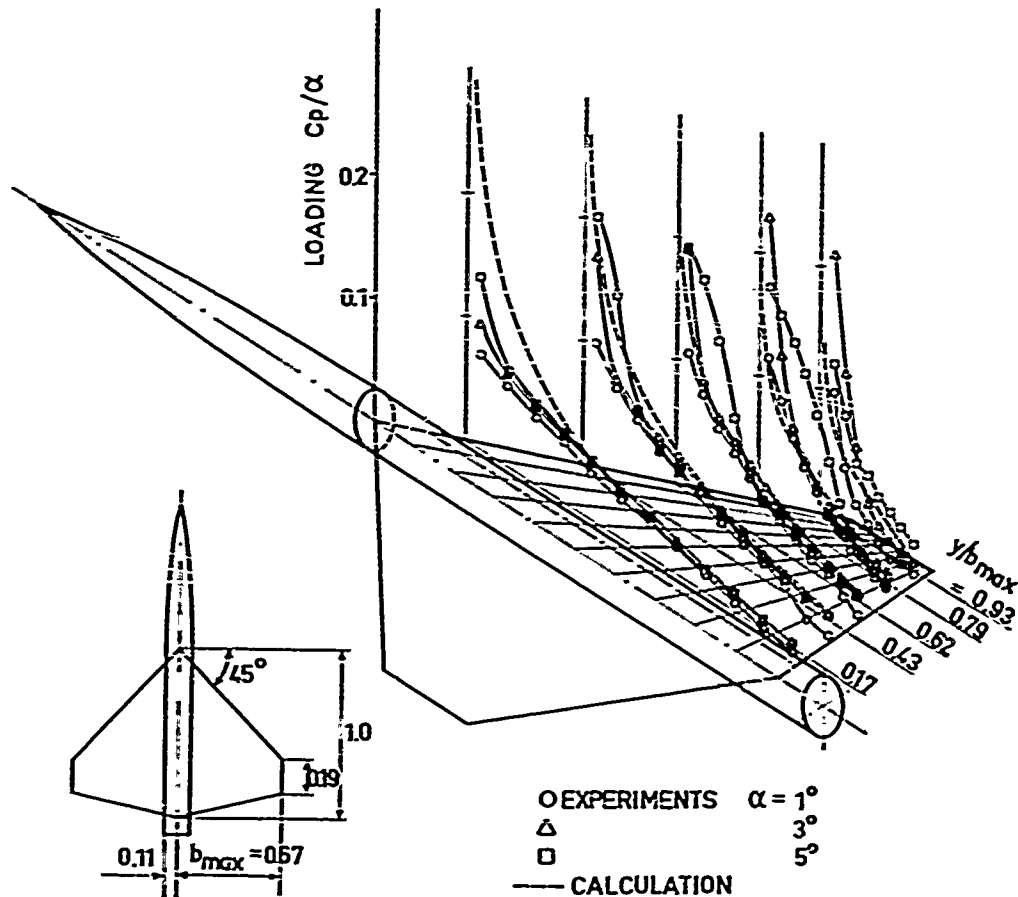
Fig. 3. Measured and calculated loading on a delta wing at $M = 0.7$.

O EXPERIMENTS $\alpha = 1°$
△ $3°$
□ $5°$
—— CALCULATION
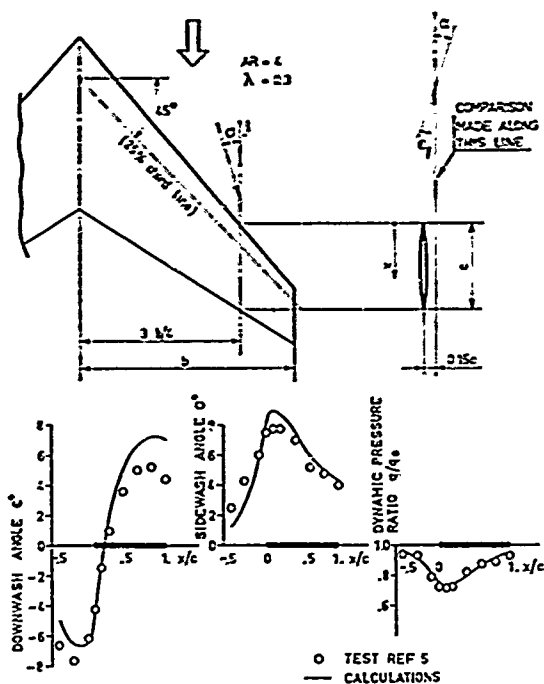
Fig. 4. Measured and calculated conditions away from the surface of a swept wing at 8.2° angle of attack.

O TEST REF 5
—— CALCULATIONS

the plane of symmetry. The loading at $\eta = 0.17$ is overestimated by the theory. For the rest of the wing the agreement between measurements and calculations is better. However, this agreement deteriorates with increasing spanwise coordinate and incidence. This discrepancy is due to the increasing strength of the free vortex over the leading edge.

The flow conditions outside the wing chord planes can also be determined. The calculated data are shown together with experimental ones in Fig. 4. From the experiments reported by Alford in Ref. 5, the effect of 8.2° angle of attack was obtained by subtracting values for zero angle of attack from values for 8.2°. The comparison is limited to one line $y = 3b/4$; $z = -0.15c$, where b is the wing semispan, and c is the local chord. In points along this line the disturbance velocities u, v and w were calculated. They are shown in the
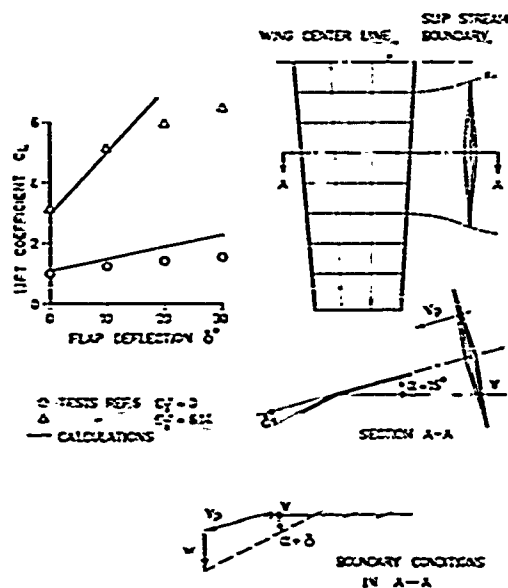
Fig. 5. Measured and calculated lift coefficients for a wing in a propeller slipstream at 15° angle of attack.

graphs as a local dynamic pressure q/q_0, sidewash angle σ, and downwash angle ε. All the flow characteristics are well predicted by the calculations except, curiously, the upwash angle under the wing.

Finally, one example with a wing in the slip stream of a propeller will be shown. The experimental data are taken from Ref. 6. The approximate layout of the wing and propeller appears in Fig. 5. The panel pattern is chosen such that some panels are completely contained inside the slipstream at a thrust coefficient $C_T' = 6.14$ and the other panels are exterior to the slipstream. The wing and propeller axis form an angle α to the free stream direction, a flap covering all the trailing edge is deflected an angle δ. The boundary condition is fulfilled in a plane parallel to the free stream velocity V. V_p is the propeller slipstream velocity. For a panel situated in the slip stream the propeller's downwash is considered, and only the vector w is contributed by the vortex system. For small angles w becomes

$$w = (\alpha + \delta)(V + V_p) - \alpha V_p$$

Fig. 5 also contains a chart that shows $C_L(\delta, C_T')$ for $\alpha = 15°$, C_T' is the propeller

thrust coefficient based on free stream velocity and wing area. It appears that a good estimate of the lift coefficient can be made, when no flow separations are present. Flap separations should increase with flap deflection and decrease with thrust coefficient.

REFERENCES

1. RUBBERT, P. E.: Theoretical characteristics of arbitrary wings by a non-planar vortex lattice method. *The Boeing Co. Report DG-9244* (1962).
2. DEYOUNG, J., HARPER, C. W.: Theoretical symmetric span loading at subsonic speeds for wings having arbitrary plan form. *NACA Rep. 921* (1948).
3. MULTHOPP, H.: Methods for calculating the lift distribution of wings (Subsonic lifting-surface theory). *Aero. Res. Counc., R & M 2884* (1955).
4. KULAKOWSKI, L. J., HASKELL, R. N.: Solution of subsonic nonplanar lifting surface problems by means of high-speed digital computers. *J. Aero/Space Sci.*, Vol. 28, No. 2 (February, 1961), pp. 103–112, 176.
5. ALFORD, W. J., JR.: Theoretical and experimental investigation of the subsonic-flow fields beneath swept and unswept wings with tables of vortex-induced velocities. *NACA TN 3738* (1956).
6. KUHN, R. E., DRAPER, J. W.: An investigation of a wing-propeller configuration employing large-chord plain flaps and large diameter propellers for low-speed flight and vertical take-off. *NACA TN 3307* (1954).

APPENDIX 1

LOCATION OF VORTICES AND CONTROL POINTS

In the two-dimensional case the vortices and control points can be so located on a straight airfoil chord that the vortex lattice gives the same lift and pitching moment as thin airfoil theory does.

Let the chord be divided into r equal parts, and let the vortex be placed a distance ξ times the part chord from its leading edge and the control point a distance η times the part chord behind the vortex. The following figure applies to the i-th part.
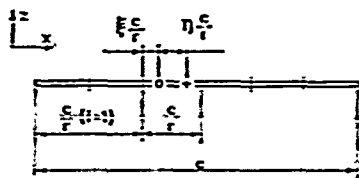
The x-coordinate for the i-th control point is x_{D_i}.

$$x_{D_i} = \frac{c}{r}[(i-1) \div \xi \div \eta]$$

The j-th vortex is positioned in x_{v_j}.

$$x_{v_j} = \frac{c}{r}[(j-1) \div \xi]$$

The velocity induced at x_{D_i} due to the vortex at x_{v_j} is w_{ij}.

$$w_{ij} = \frac{\Gamma_j \cdot r}{2\pi c \cdot (i - j \div \eta)}$$

The distribution of induced velocities is related to the vortex distribution by a set of linear equations.

$$\{w\} = \frac{r}{2\pi c} \cdot \left[\frac{1}{i-j \div \eta}\right]\{\Gamma\}$$

Insert this equation into the equation for the total lift of the airfoil.

$$L = \varrho V \cdot [1]\{\Gamma\} = \varrho V \frac{2\pi c}{r} \cdot [1]\left[\frac{1}{i-j \div \eta}\right]^{-1}\{w\}$$

Likewise an expression for the moment is obtained

$$M = \varrho V \cdot [x_v]\{\Gamma\} = \varrho V \frac{2\pi c}{r} \cdot [j - 1 \div \xi]$$

$$\times \left[\frac{1}{i-j \div \eta}\right]^{-1}\{w\}$$

From thin airfoil theory the lift and moment are known.

$$L = \tfrac{1}{2}\varrho V^2 \cdot c \cdot 2\pi \cdot w/V$$

$$M = L \cdot c/4$$

After identification of the two equations for L and M respectively, η and ξ can be solved.

$$\left.\begin{aligned} 1 &= \frac{2}{r} \cdot [1]\left[\frac{1}{i-j \div \eta}\right]^{-1}\{1\} \\ 1 &= \frac{8}{r^2} \cdot [j - 1 \div \xi]\left[\frac{1}{i-j \div \eta}\right]^{-1}\{1\} \end{aligned}\right\} \text{(A 1.1)}$$

The inversions have only been performed for $r = 2,3$.

$$r = 2; \quad \left[\frac{1}{i-j \div \eta}\right]^{-1} = \eta\begin{bmatrix} 1-\eta^2, & \eta(\eta \div 1) \\ \eta(\eta-1), & 1-\eta^2 \end{bmatrix}$$

$$r = 3; \quad \left[\frac{1}{i-j \div \eta}\right]^{-1}$$

$$= \eta\begin{bmatrix} \dfrac{(\eta^2-4)(\eta^2-1)}{4}, & -\dfrac{\eta(\eta^2-1)(\eta \div 2)}{2}, \\[2mm] \dfrac{\eta(\eta \div 1)^2(\eta \div 2)}{4} \\[2mm] -\dfrac{\eta(\eta^2-1)(\eta-2)}{2}, & (\eta^2-1)^2, \\[2mm] -\dfrac{\eta(\eta^2-1)(\eta \div 2)}{2} \\[2mm] \dfrac{\eta(\eta-1)^2(\eta-2)}{4}, & -\dfrac{\eta(\eta^2-1)(\eta-2)}{2}, \\[2mm] \dfrac{(\eta^2-1)(\eta^2-4)}{4} \end{bmatrix}$$

The solutions for η and ξ are

$$\eta = \tfrac{1}{2}, \quad \xi = \tfrac{1}{4}$$

if $r = 1, 2, 3$. These η- and ξ-values numerically satisfy Eq. (A1.1) for useful values of r.

The same vortex and control point positions, i.e. $\xi = \tfrac{1}{4}$, $\eta = \tfrac{1}{2}$, have been chosen also for the three-dimensional case. Calculations with different panel patterns for one wing planform have given very consistent values of lift coefficient and center of pressure, which is shown in the table on P. 10 and in Fig. 2. The suggested locations are therefore thought to be very useful approximations.

APPENDIX 2

DIVISION OF THE LIFTING SURFACE INTO PANELS

Let the real planform be approximated with a number of trapezoids. In Fig. A2.1 three trapezoidal wing parts represent starboard half of the wing. The parts are defined by the coordinates a, b, c. Each wing part is divided in the spanwise and chordwise direction to form q columns and r rows of panels.

Fig. A2.1 shows that the interval $b_k \leqslant y \leqslant b_{k+1}$ is divided at stations $y = c_{k,l}$, and that the chordwise division is made by straight lines between the points $(a_k \div d_{k,m} \cdot c_k, b_k)$ and $(a_{k+1} \div d_{k+1,m} \cdot c_{k+1}, b_{k+1})$. In this way the wing parts are divided into wing panels.

It is convenient to have the panels numbered. The following system may be used. Panel number 1 is the panel in the first wing part's first column and first row. Number 2 stands for the panel in the first column and second row, and so on. r becomes the number of the panel in the last row. The first panel in the second column has number $r \div 1$. The last panel of the first wing part is qr. The numbers for the other wing parts follow after qr. The number i of a panel is obtained from its location in the wing part k, panel column l, and panel row m

$$i = m \div (l-1)r_k \div \sum_{j=1}^{k-1} q_j r_j$$

where q_j and r_j are the total number of columns and rows, respectively, for wing part j.
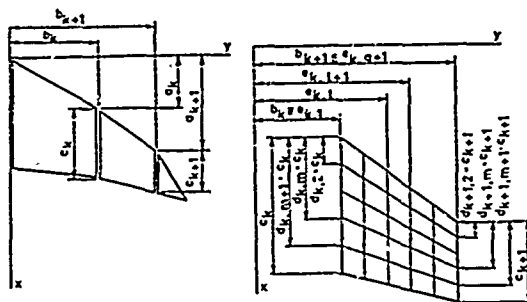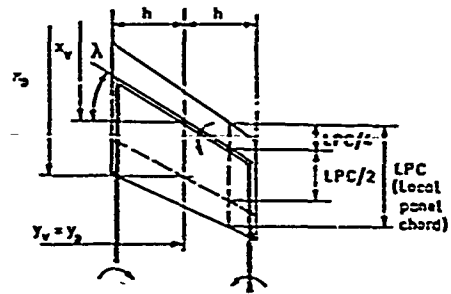

Fig. A2.1. Wing parts and panels.

Fig. A2.2. Wing panel with horseshoe vortex and control point.

The following set of equations can be used for obtaining the quantities that specify the vortices x_V, y_V, h, λ and the control points x_D, y_D from the quantities that determine the panels a, b, c, d, and e. Fig. A2.2 illustrates the variables for vortices and control points.

$$y_V = y_D = (c_{k,l} \div c_{k,l+1})/2$$

$$x_V = a_k \div c_k \cdot (3d_{k,m} \div d_{k,m+1})/4 \div (y_V - b_k) \cdot \operatorname{tg}\lambda$$

$$x_D = a_k \div c_k \cdot (d_{k,m} \div 3d_{k,m+1})/4$$
$$\div [c_{k+1} \cdot (d_{k+1,m} \div 3d_{k+1,m+1})/4$$
$$- c_k \cdot (d_{k,m} \div 3d_{k,m+1})/4 \div a_{k+1} - a_k]$$
$$\times (y_V - b_k)/(b_{k+1} - b_k)$$

$$h = (e_{k,l+1} - e_{k,l})/2$$

$$\operatorname{tg}\lambda = [c_{k+1} \cdot (3d_{k+1,m} \div d_{k+1,m+1})/4$$
$$- c_k(3d_{k,m} \div d_{k,m+1})/4$$
$$\div a_{k+1} - a_k]/(b_{k+1} - b_k)$$

APPENDIX 3

THE INFLUENCE COEFFICIENTS P, Q, R

The horseshoe vortex is positioned in a plane $z = \text{const.}$ with the bound vortex forming an angle to the y-axis and the trailing vortices parallel to the x-axis. The geometry is obtained from the real wing in a Mach number M air stream through a Prandtl-Glauert transformation, that is the y and z coordinates are multiplied by β, $\beta = \sqrt{1 - M^2}$.
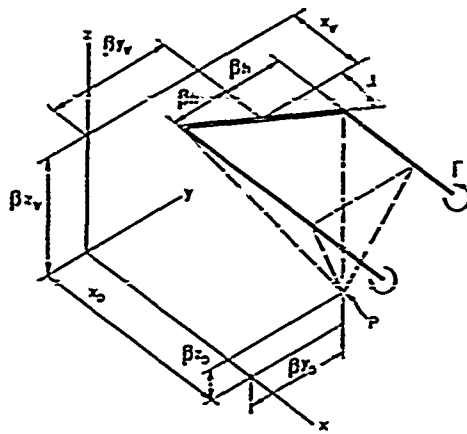
Fig. A3.1. The transformed vortex.

The three disturbance velocity components at the point $(x_D, \beta y_D, \beta z_D)$ due to a horseshoe vortex of intensity Γ and with the geometry defined by the coordinates $(x_v, \beta y_v, \beta z_v)$ and the dimensions βh and μ will be calculated by Biot-Savart's law.

The *bound vortex* forms part of the line

$$\operatorname{tg}\mu\beta\cdot(y-y_v) = x-x_v, \quad z = \beta z_v.$$

A straight line vortex induces velocities that lay in planes normal to the vortex. The induced velocity in a point P is also normal to the straight line, which connects P and the vortex. Fig. A3.2 shows the line vortex between Q and R and the induced velocity vector in P. PS is the line through P normal to the vortex. $P'S$ is the projection of that line on the plane $z = \beta z_v$. The equation for $P'S$ is
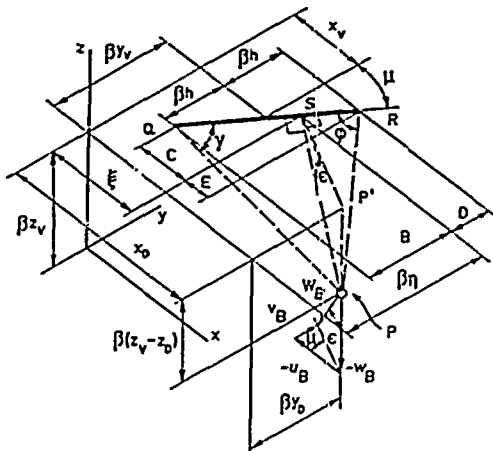
$$-\beta\cdot(y-y_D)/\operatorname{tg}\mu = x - x_D$$

Fig. A3.2. The bound vortex.

This determines the point of intercept S $(\xi, \beta\eta, \beta z_v)$.

$$\xi = \frac{x_v + x_D \operatorname{tg}^2\mu + \beta\cdot(y_D-y_v)\operatorname{tg}\mu}{\operatorname{tg}^2\mu + 1}$$

$$\beta\eta = \frac{\beta y_D + \beta y_v \operatorname{tg}^2\mu + (x_D-x_v)\operatorname{tg}\mu}{\operatorname{tg}^2\mu + 1}$$

W_B will denote the velocity induced in P by the bound vortex.

$$W_B = \frac{\Gamma(\cos\gamma + \cos\varphi)}{4\pi\sqrt{A^2 + Z^2}}$$

$$\cos\gamma = \frac{\overline{QS}}{\overline{QP}} = \frac{\pm\sqrt{B^2 + C^2}}{\sqrt{A^2 + B^2 + C^2 + Z^2}}$$

$$\cos\gamma > 0 \quad \text{for} \quad \eta > y_v - h$$

$$\cos\gamma < 0 \quad \text{for} \quad \eta < y_v - h$$

$$\cos\varphi = \frac{\overline{RS}}{\overline{RP}} = \frac{\pm\sqrt{D^2 + E^2}}{\sqrt{A^2 + D^2 + E^2 + Z^2}}$$

$$\cos\varphi < 0 \quad \text{for} \quad \eta > y_v + h$$

$$\cos\varphi > 0 \quad \text{for} \quad \eta < y_v + h$$

$$A^2 = (\overline{SP'})^2 = (x_D-\xi)^2 + \beta^2\cdot(\eta-y_D)^2$$

$$B = \beta\cdot(\eta-y_v+h)$$

$$C = \xi-x_v + \beta h\operatorname{tg}\mu$$

$$D = \beta\cdot(y_v+h-\eta)$$

$$E = x_v + \beta h\operatorname{tg}\mu - \xi$$

$$Z = \beta\cdot(z_v-z_D)$$

The disturbance velocity W_B is resolved into its components along the coordinate axis u_B, v_B, w_B

$$u_B = -W_B\sin\varepsilon\cos\mu$$

$$v_B = W_B\sin\varepsilon\sin\mu$$

$$w_B = -W_B\cos\varepsilon$$

$$\sin\varepsilon = \frac{Z}{\sqrt{A^2+Z^2}}$$

$$\cos\varepsilon = \frac{\pm A}{\sqrt{A^2+Z^2}} \qquad \begin{array}{l} \cos\varepsilon > 0 \quad \text{for} \quad x_D > \xi \\ \cos\varepsilon < 0 \quad \text{for} \quad x_D < \xi \end{array}$$

The *port free vortex* and the velocity vector W_P induced at P are shown in Fig. A3.3.

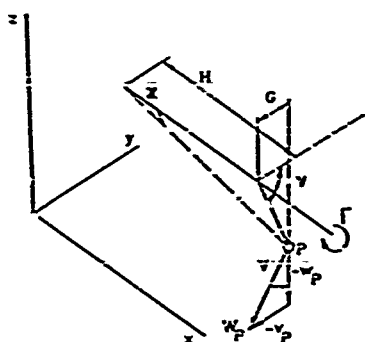$$W_P = \frac{\Gamma}{4\pi}\cdot\frac{1+\cos\cdot}{\sqrt{G^2+Z^2}}$$

Fig. A3.3. Port free vortex.

$$\cos \varkappa = \frac{H}{\sqrt{G^2 + H^2 + Z^2}}$$

$$G = \beta \cdot (y_D - y_V + h)$$

$$H = x_D - x_V + \beta h \, \mathrm{tg} \, \mu$$

The components of velocities along the coordinate axis are u_P, v_P, and w_P.

$$u_P = 0$$

$$v_P = - W_P \sin r$$

$$w_P = - W_P \cos r$$

$$\sin r = \frac{Z}{\sqrt{G^2 + Z^2}}$$

$$\cos r = \frac{G}{\sqrt{G^2 + Z^2}}$$

The velocities W_S due to the *starboard free vortex* are obtained similarly.
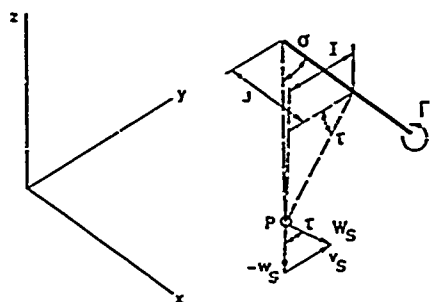

Fig. A3.4. Starboard free vortex.

$$W_S = \frac{\Gamma}{4\pi} \frac{\cos \sigma + 1}{\sqrt{I^2 + Z^2}}$$

$$\cos \sigma = \frac{J}{\sqrt{I^2 + J^2 + Z^2}}$$

$$I = \beta(y_V + h - y_D)$$

$$J = x_D - x_V - \beta h \, \mathrm{tg} \, \mu$$

The components of W_S along the axis are u_S, v_S, and w_S.

$$u_S = 0$$

$$v_S = W_S \sin \tau$$

$$w_S = - W_S \cos \tau$$

$$\sin \tau = \frac{Z}{\sqrt{I^2 + Z^2}}$$

$$\cos \tau = \frac{I}{\sqrt{I^2 + Z^2}}$$

The complete horseshoe vortex causes a disturbance velocity with the components u, v, w

$$u = u_B + u_P + u_S$$

$$v = v_B + v_P + v_S$$

$$w = w_B + w_P + w_S$$

$$
\left.
\begin{aligned}
u &= -\frac{\Gamma}{4\pi} \frac{\cos \gamma + \cos \varphi}{A^2 + Z^2} Z \cos \mu = P\Gamma \\[2mm]
v &= \frac{\Gamma}{4\pi} \left[\frac{\cos \gamma + \cos \varphi}{A^2 + Z^2} \sin \mu - \frac{1 + \cos \varkappa}{G^2 + Z^2} \right. \\
  &\quad \left. + \frac{\cos \sigma + 1}{I^2 + Z^2} \right] Z = Q\Gamma \\[2mm]
w &= \frac{\Gamma}{4\pi} \left[\mp \frac{\cos \gamma + \cos \varphi}{A^2 + Z^2} \cdot A - \frac{1 + \cos \varkappa}{G^2 + Z^2} G \right. \\
  &\quad \left. - \frac{\cos \sigma + 1}{I^2 + Z^2} I \right] = R\Gamma
\end{aligned}
\right\} \quad (A\,3.1)
$$

The rule of signs for the first term in w is: use minus when $x_D > \xi$, use plus when $x_D < \xi$.

APPENDIX 4

EFFECT OF WING ELASTICITY

Eq. (4) yields the distribution of angle of attack that corresponds to a given loading. The obtained angles for the loaded wing, ω_Q, are the same, whether the wing is rigid or elastic. However, when the elastic wing is unloaded, it will in general change its shape. The corresponding change in streamwise angle will be denoted $\Delta \omega$. It is often of interest to know the distribution of angle of attack for the unloaded elastic

wing, ω_0. Mostly ω_0 is the input for the calculation of the loading of an elastic wing.

$$\{\omega_a\} = \{\omega_o\} + \{\Delta\omega\}$$

The angle of deformation is obtained from a deformation matrix $[D]$ of the structure and the load vector $\{l\}$ for the deformed wing

$$\{\Delta\omega\} = [D]\{l\}$$

The load vector is found from Eqs. (5) and (9).

$$-\{l\} = \frac{4q}{\beta} \cdot \left[\diagdown h \diagdown \right] [S_1]^{-1}\{\omega_0\}$$

A combination of these equations gives the unloaded wing angle of attack distribution

$$\{\omega_0\} = \left[\left[\diagdown 1 \diagdown \right] + \frac{4q}{\beta} \cdot [D]\left[\diagdown h \diagdown \right][S_1]^{-1} \right]\{\omega_0\}$$

$$(A4.1)$$

The loaded wing angle of attack distribution is obtained from Eq. (A4.1)

$$\{\omega_0\} = \left[\left[\diagdown 1 \diagdown \right] + \frac{4q}{\beta} \cdot [D]\left[\diagdown h \diagdown \right][S_1]^{-1} \right]^{-1}\{\omega_0\}$$

$$(A4.2)$$

Inserting Eq. (A4.2) into Eq. (5) gives an equation for calculation of loadings for elastic wings.